Materials Transactions, Vol. 43, No. 4 (2002) pp. 751 to 756

EXPRESS REGULAR ARTICLE

Effect of Surface Finishes on Ball Shear Strength in BGA Joints with Sn–3.5 mass%Ag Solder

Chang-Bae Lee *1, In-Young Lee, Seung-Boo Jung *2 and Chang-Chae Shur

Department of Advanced Materials Engineering, Sungkyunkwan University, 300 Chunchun-dong, Jangan-ku, Suwon 440-746, Korea

The present study is aimed at the assessment on the reliability of solder ball attachment to the bond pads of BGA substrate with various plating schemes. The reliability of solder ball attachment is characterized by mechanical ball shear tests. In addition to the ball shear tests, SEM is performed to inspect the cross-section and the fracture surface of the tested specimens for failure analysis. The aging was conducted in convection ovens in air at 343, 393, 423 and 443 K respectively for times ranging 8.64×10^4 to 864×10^4 s. Without regard to the deposited layer, the shear strength of BGA joints decreased with the increasing temperature and time. After isothermal aging, the fracture surface shows various characteristics depending on aging temperature and time, and the types of BGA pad.

(Received October 16, 2001; Accepted February 25, 2002)

Keywords: *ball shear test, reliability, fracture surface, ball grid array (BGA) joint, isothermal aging*

1. Introduction

Soldering is the preferred method for attaching components to printed circuit boards(PCB) in electrical and electronic devices.[1,2] The ball grid array(BGA) package has been successfully applied to many electronic products.[3–6] For solder ball-grid-array technology, solder joint reliability is one of the most critical issues in the development of the technologies.[7,8] Nickel-based metallization is the currently focused scheme for microelectronics packaging to prevent excessive intermetallic compound formation during packaging, and in service condition.[9] The contact pads for the solder balls on the BGAs usually have the Au/Ni surface finish. Each layer of the metal plated on BGA substrates has its own specific functions. Nickel layer is used as a barrier to prevent copper from diffusing into solder balls because copper will interact with tin to form Cu–Sn intermetallic compound. This intermetallic compound will then affect the shear strength of solder balls. Gold is plated on Ni surface of the ball pads not only to improve the wettability, but also to increase resistance to corrosion.[10,11]

An increasing number of higher density BGA substrates require electroless surface finishes for feature size and routability. The use of immersion Au/electroless Ni as an alternative surface finish for area array packages and printed circuit board (PCB) is increasing to meet the requirements of the increased density and electrical performance.[12,13] This trend is continuing despite the evidence that immersion Au/electroless Ni causes or contributes to catastrophic, brittle, and interfacial solder joint fractures.[14–16] The electroless plating defect is manifested as brittle fracture at the interface between the Ni deposits and the intermetallic compound. The package surface finish is the important package variable, which is influencing the fracture mode. Ball shear testing is the most common test method used for assessing solder ball attachment quality on area array packages.[17]

The objective of the present study is to investigate the effect of various plating schemes on the reliability of BGA solder joints. In the present study, the shear strength of solder balls on BGA substrates with three different surface finishes is studied. Shear tests are also conducted as a function of the time and temperature for isothermal aging. The results are discussed in terms of accurate interpretation of shear test data and suggestions are made for guidelines for ball shear test requirements.

2. Experimental Procedures

Solder balls used in this study were eutectic Sn–3.5 mass%Ag solder with a diameter of 760 μm. The BGA substrates used in this study were commercially available, and thermally enhanced BGA substrates with 421 pads, with each pad having a diameter of 640 μm. The shear strengths of solder balls on BGA pads were measured with three different surface finishes, namely, bare Cu pad, electroless Ni–P/Cu pad with Ni–P layer thickness of 7–8 μm, and immersion Au/electroless Ni–P/Cu pad with Ni–P and Au layers of 0.15 and 7–8 μm thickness respectively. The Ni–P and Au layers were electroless plated on the BGA Cu pad, and the thickness of the layers was examined by scanning electron microscopy (SEM). The electroless Ni plating deposits a mixture of Ni and phosphorous and not pure Ni, because of the use of hypophosphite in the chemical reaction for reducing Ni ions. Electroless Ni layers which contain 15 at%P have an amorphous structure. The temperature of the Ni bath is 361 K and the pH 4.3–4.8. A thin Au layer is deposited on the Ni using an immersion Au bath to prevent the oxidation of Ni. The temperature of the Au bath is 362 K and the pH 5.6–6.2. The solder balls were dipped into flux and then planted on the pads manually and the balls were reflowed by using a IR reflow oven. The peak reflow temperature, the highest temperature a package experienced, was 523 K and the reflow time at which solder balls melt was 120 s. Solder joints were cross-sectioned for examination directly after being reflowed and after being aged in a furnace at 343, 393, 423, and 443 K

*1Graduate Student, Sungkyunkwan University.
*2Corresponding author, E-mail: sbjung@yurim.skku.ac.kr

respectively for times ranging from 8.64×10^4 to 864×10^4 s. The aging was conducted in convection ovens in air, with the temperature controlled to within ± 1 K for the given test duration. In order to examine the fracture surface and cross sections of all specimens were observed with a secondary electron image (SEI) and backscattered electron image (BEI) by the SEM. Backscattered electron image was used to obtain the micrographs to produce better contrast among various phase. The composition of each phase was determined using the energy-dispersive X-ray (EDX) analysis. Ball shear tests as a function of time, temperature and three types surface finishes were performed. For each read point, three packages were made for the predetermined time and ten balls were sheared off of each sample, making each read point an average of thirty sheared balls. The solder joint shear strength was measured by ball shear test machine. The blade height was set at 10 μm and the shearing speed was maintained of at 100 μm/s.

3. Results and Discussion

In the present study, mechanical shear tests were employed to characterize the strength of solder balls attached to the bond pads of BGA substrates. Such ball shear strength is considered as an index for solder joint reliability.

Figure 1 shows the variation of shear strength of the solder balls with the time and temperature, and various types of BGA pad surface finishes (bare Cu, electroless Ni–P/Cu and immersion Au/electroless Ni–P/Cu pads). The shear strength decreased with the increasing temperature and time irrespective of the deposited layer. The results, which are presented in Fig. 1, show that as the aging time increased, the shear strength of the parts steadily decreased after the first few read points. On BGA Cu pads, the shear strength of the balls aged at 393, 423, and 443 K for 129.6×10^4 s decreased more rapidly than that aged at 343 K. The shear strength decreased with increasing temperature and with immersion Au/Ni–P/Cu, bare Cu pad and electroless Ni–P/Cu pads in order. A significant decrease in shear strength was noticed except the strengths at 343 K on plated pads after 129.6×10^4 s of isothermal aging. It can be seen from the test result, that the shear strengths decrease by 17.75, 17.01 and 27.03% after 864×10^4 s of aging at 423 K compared to the strengths measured after as-reflowed for Cu pad, electroless Ni–P/Cu pad and immersion Au/Ni–P/Cu pads. Especially the shear strength for immersion Au/Ni–P/Cu pads decreased sharply with increasing time and temperature as shown in Fig. 1(c). It was noticed that the shear strength for both electroless Ni–P/Cu and bare Cu pads was consistently higher than that of the immersion Au/Ni–P/Cu pads for all aging times. The shear strengths of as-reflowed condition were measured as 172.33, 172.03 and 159.59 mN for Cu pad, electroless Ni–P/Cu pad and immersion Au/Ni–P/Cu pads, respectively. But after aging at 423 K for 864×10^4 s, the shear strengths were decreased to 141.74, 142.76 and 116.45 mN for the above pads. As test goes on, the shear strength of the solder ball decreases approximately parabolic with the duration of the test for all three types of BGA pads. During aging at 343 K, there is relatively little change in the shear strength with aging time as shown in Fig. 1. As the temperature (343 K) corresponds

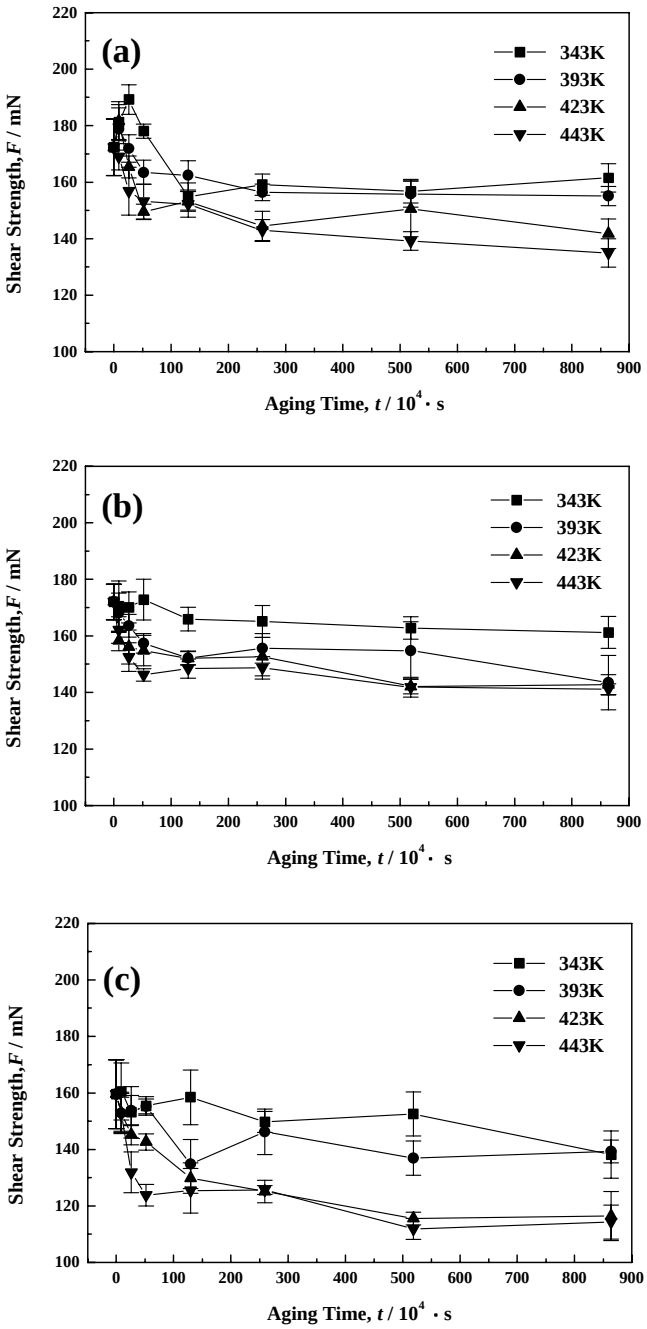

Fig. 1 Variations of the ball shear strength with aging time and temperature: (a) Cu pad, (b) electroless Ni–P/Cu pad and (c) immersion Au/Ni–P/Cu pad.

a relatively low homologous temperature of the solder, the microstructure of solder at the temperature (343 K) is more stable than that of solder at different temperatures (393, 423 and 443 K). As shown in Fig. 1, it can be clearly seen that initial aging increased the shear strength of solder joint at 343 K. The increase of ball shear strength after initial aging could be attributed to the transformation of solder microstructure from a dendritic structure to more uniform distribution of Ag_3Sn dispersoids (see Figs. 2(a) and (b)). As a consequence, this transformation resulted in an increment of solder strength. This is analogous to the fact that the coarsened microstructure exhibits lower shear strength as compared to fine grain structure. Further aging resulted in coarsening of the grain

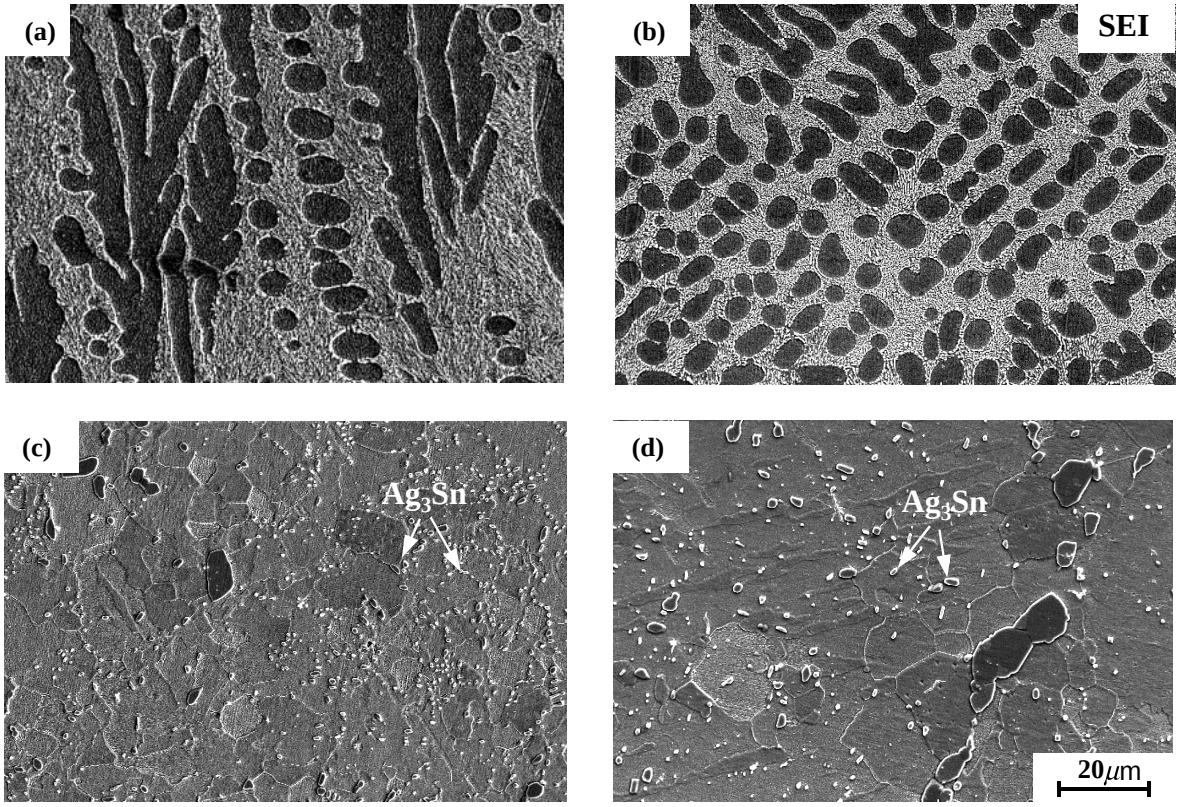

Fig. 2 SEM micrographs of Sn–3.5Ag solder after aging: (a) as-reflowed (b) 343 K, 51.84×10^4 s (c) 423 K, 259.2×10^4 s and (d) 423 K, 864×10^4 s.

structure and the reduction of shear strength (see Figs. 2(c) and (d)). After isothermal aging, the fracture surface shows various characteristics depending on aging temperature, aging time and the types of BGA pad.

Figure 3 shows the fracture surface of BGA Cu, electroless Ni–P/Cu and immersion Au/Ni–P/Cu pad with Sn–3.5Ag solder before and after aging at 423 K for 864×10^4 s. From Figs. 2(c) and (d), the grain size has increased considerably during the isothermal aging and is suggested to be the main cause of the reduced shear strength. For Cu BGA pad, the ball shear initially occurred through the solder layer but changed to brittle fracture at the interface between the solder ball and the intermetallic region, within the Cu_6Sn_5 intermetallic layer after aging at 423 K for 864×10^4 s. For electroless Ni–P/Cu BGA pad, all failures were observed within the solder bulk side and not at the interface. The fracture surfaces with electroless Ni–P/Cu pads showed more ductile fracture mode than those of Cu and immersion Au/Ni–P/Cu pads. For immersion Au/Ni–P/Cu BGA pads, after long aging times, the fracture mechanism changes from ductile fracture in solder to brittle interfacial fracture.

Figure 4 shows the fracture surface for Cu BGA pad joint with its EDX analysis after aging at 423 K for 864×10^4 s. The fracture occurs at the interface between solder and Cu_6Sn_5 intermetallic, within the Cu_6Sn_5 intermetallic. From the results of EDX analysis, the Cu_6Sn_5 and Ag_3Sn were detected. Failure mode for Cu BGA pad joint is a combination of (i) brittle fracture at the interface between solder and Cu_6Sn_5 intermetallic, brittle fracture within the Cu_6Sn_5 intermetallic and (ii) the ductile fracture inside of solder.

Figure 5 shows the cross sectional SEM micrographs of the interface between solder and Cu pad aged at 423 K for 864×10^4 s. The composition of each Cu–Sn intermetallics and Ag–Sn particles were verified by EDX analysis as shown in Fig. 5. The aged solder joint comprises of the Cu pad, Cu_3Sn and Cu_6Sn_5 intermetallic layers, Ag_3Sn intermetallics embedded within the Cu_6Sn_5 intermetallic layer, Ag_3Sn intermetallics in the solder, and the Sn-rich phase. Under high magnification, it was found that the Cu_6Sn_5 intermetallic growth involved the inclusion of Ag_3Sn. As the Cu_6Sn_5 intermetallic layer grew toward the solder during isothermal aging, Ag_3Sn intermetallic located near the solder/intermetallic interface incorporated into the Cu_6Sn_5 intermetallics. The result of EDX showed that Cu_6Sn_5 and Cu_3Sn intermetallic layers did not appear to have dissolved Ag within them. Based on the above analysis, we conclude that the brittle fracture was caused by the combination of the brittle property (Cu_6Sn_5) and microstructural misfit (Cu_6Sn_5/Ag_3Sn). Also, no cracked Ag_3Sn was found on fracture surface as shown in Fig. 4. This indicates that the boundaries between Cu_6Sn_5 and Ag_3Sn are weaken due to the decohesion between Cu_6Sn_5 and Ag_3Sn.

Figure 6 shows the fracture surface for immersion Au/Ni–P/Cu BGA pad joint with its EDX analysis after aging at 423 K for 864×10^4 s. In as-reflowed condition, the fracture occurred mainly through the bulk solder as shown in Fig. 3(e). But, after isothermal aging at 423 K for 864×10^4 s, the fracture was found along the interfaces of the Ni_3Sn_4 and $Ni_{67.21}Sn_{17.36}P_{15.43}$ (hereafter Ni–Sn–P), the Ni–Sn–P and P-rich Ni layer, the solder ball and Ni_3Sn_4 intermetallics, and within the Ni_3Sn_4 intermetallics. Dimples are also found in the fracture surface and the Ni_3Sn_4 intermetallic compound particles can be seen clearly at the center of each dimple. Af-

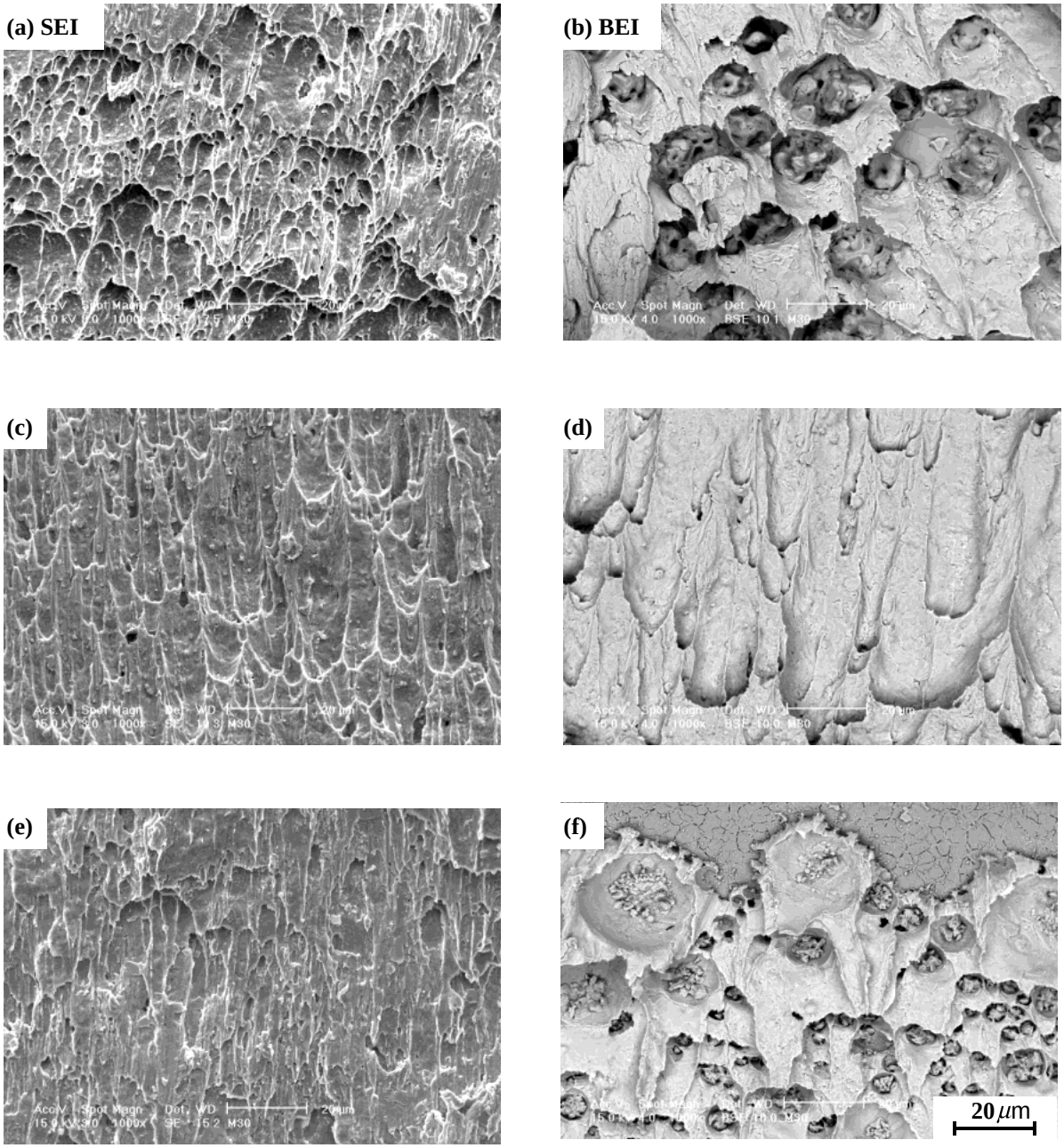

Fig. 3 Fracture surface after ball shear test for solder/Cu pad joint (a, b), solder/electroless Ni–P/Cu pad joint (c, d), and solder/immersion Au/Ni–P/Cu joint (e, f): as-reflowed (a, c, and e) and after aging at 423 K for 864×10^4 s (b, d, and f).

ter isothermal aging, no Au was ever found to remain on the surface of BGA pad, since all the Au dissolved into the molten solder during soldering. In addition, because of the limited amount of Au concentration, in the solder and solder/pad interface, Au or Au–Sn intermetallics may not be observed. Ductility loss of Sn base solder due to the presence of gold is often quoted as gold embrittlement and cited as a reason for failure of solder joints.[18] In this study, although Au was not found on fracture surface, the decrease of shear strength may be due to the gold embrittlement. In other words, the gold embrittlement in BGA joints occurred at much lower Au concentration. After isothermal aging, a P-rich Ni layer was formed at the interface between Ni–Sn–P and Ni–P deposits layer, and fracture at this layer was not the dominate failure site for immersion Au/Ni–P/Cu pad. The deterioration of solder ball shear strength was found to be mainly caused by the interfacial fracture between Ni_3Sn_4 and Ni–Sn–P compound, within the Ni_3Sn_4 intermetallic compound and gold embrittlement.

Figure 7 shows the SEM micrographs of the interface between solder and immersion Au/Ni–P/Cu pad after aging at 423 K for 864×10^4 s. Back-scattered electron imaging of SEM was used to provide more distinguishable boundaries of the interfacial intermetallic layer. In the results of EDX analysis, three intermetallic layers were observed between the solder and Ni–P deposit. The P-rich Ni layer with an embedded cavity was found adjacent to Ni–P deposits. Ni_3Sn_4 intermetallic was detected between the P-rich Ni layer and solder. Also, another layer with Ni–Sn–P was observed between P-rich Ni layer and Ni_3Sn_4 intermetallic layer. From solder to the BGA pads, the structure of the solder joint consists of a bulk solder, Ni_3Sn_4 intermetallic layer, Ni–Sn–P

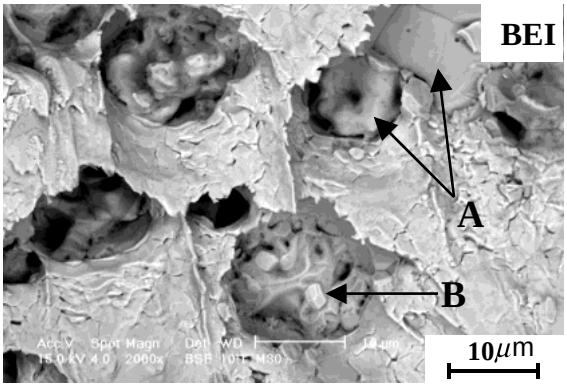

Analysis	Composition (at %)		
	Cu	Sn	Ag
A	54.69	45.31	—
B	—	26.23	73.77

Fig. 4 Fracture surface of Sn–3.5Ag/Cu pad joint after aging at 423 K for 864×10^4 s, and EDX analysis results. (A = Cu_6Sn_5, B = Ag_3Sn).

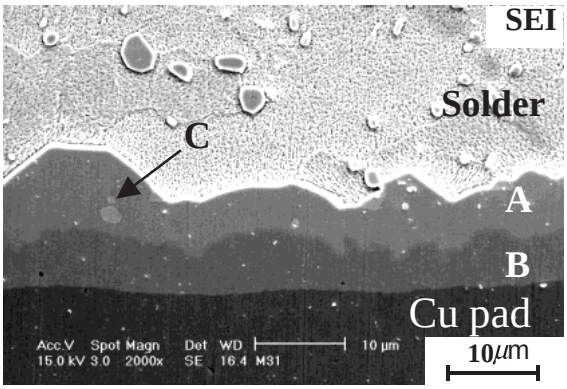

Analysis	Composition (at %)		
	Cu	Sn	Ag
A	54.18	45.82	—
B	74.20	25.80	—
C	—	25.90	74.10

Fig. 5 SEM micrograph of the intreface between Sn–3.5Ag solder and Cu pad after aging at 423 K for 864×10^4 s, and EDX analysis results. (A = Cu_6Sn_5, B = Cu_3Sn, and C = Ag_3Sn).

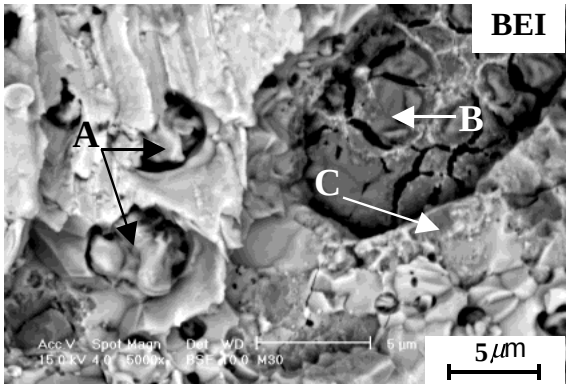

Analysis	Composition (at %)		
	Ni	Sn	P
A	43.13	56.87	—
B	74.18	—	25.82
C	67.21	17.36	15.43

Fig. 6 Fracture surface of Sn–3.5Ag solder/immersion Au/Ni–P/Cu joint after aging at 423 K for 864×10^4 s, and EDX analysis results. (A = Ni_3Sn_4, B = P-rich Ni layer and C = $Ni_{67.21}Sn_{17.36}P_{15.43}$).

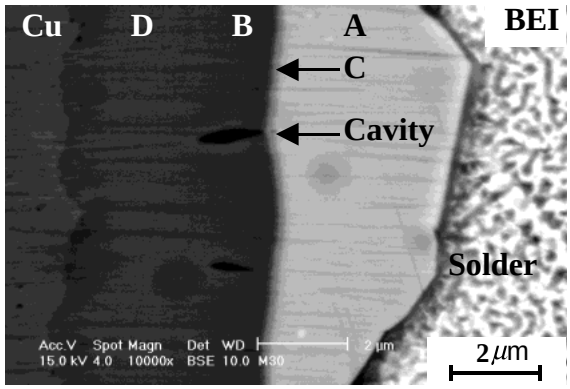

Analysis	Composition (at %)		
	Ni	Sn	P
A	43.62	56.38	—
B	74.36	—	25.64
C	67.21	17.36	15.43
D	84.69	—	15.31

Fig. 7 Backscattered electron micrograph of the interface between Sn–3.5Ag solder and immersion Au/Ni–P/Cu pad after aging at 423 K for 864×10^4 s, and EDX analysis results. (A = Ni_3Sn_4, B = P-rich Ni layer, C = $Ni_{67.21}Sn_{17.36}P_{15.43}$ and D = Ni–15 at% P).

layer, P-rich Ni layer, an amorphous Ni layer with 15 at% phosphorous, and Cu pad. During soldering, Au dissolves into the molten solder, exposing the underneath Ni and P. The Ni atoms diffused inward into the solder,[19,20] forming only a Ni–Sn intermetallics and no intermetallic compounds of Sn–P or Ag–P formed, P is expelled from the Ni–Sn intermetallic layer, and only after a long reaction period, a Ni–Sn–P was observed. During the aging, it was well known that Au atoms were diffused back to the interface between solder and Ni_3Sn_4 intermetallic and resulted in the decreasing of bonding strength.[11,14] But Au was not found remaining at the interface of BGA pad and solder ball due to the limited spatial resolution of the SEM. Although there is no Au–Sn intermetallics was found in this case, Au–Sn intermetallics must have formed at the interface between Ni_3Sn_4 intermetallics and solder. Z. Mei *et al.*[14] reported that Au–Sn intermetallic caused embrittlement in BGA joints. In this study, if Au layer completely dissolved into the molten solder during soldering, the concentration of Au in bulk solder was less than 0.10 mass%. A possible explanation is that the Au–Sn intermetallics are too rare to detect, since the Au plating is so thin for immersion Au/Ni–P/Cu BGA pads. Further work is required to fully characterize the role of Au to the degradation of shear strength. Because of the spatial and limitations of SEM and EDS, other techniques such as TEM (Transmission electron microscopy) and SAM (Scanning auger microscopy) could provide more accurate information.

4. Conclusion

The fracture surface and the ball shear strength of Sn–3.5Ag solder balls on BGA pads with three different surface finishes have been investigated. The results are summarized as follows:

(1) Without regard to the deposited layer, the shear strength decreases with the increasing temperature and time. The shear strength decreases in this order: immersion Au/Ni–P/Cu pad, bare Cu pad, and electroless Ni–P/Cu pads.

(2) The deterioration of solder ball shear strength was found to be mainly caused by the formation of intermetallic compound layers, together with the microstructure coarsening. During the aging, the failure mode gradually changes from ductile fracture in solder to brittle fracture (i) at the interface between solder and intermetallic compound, (ii) within the intermetallic compound and (iii) between two intermetallic compound layers. However, the failure mode of solder ball with electroless Ni–P/Cu pads is different from Cu pad and immersion Au/Ni–P/Cu pad. After long aging times, all failures are observed as only the ductile fracture in solder ball.

(3) The structure of solder/immersion Au/Ni–P/Cu BGA pad interface after aging at 423 K for 864×10^4 s, from solder to the BGA pads, consists of a bulk solder, Ni_3Sn_4 intermetallic layer, Ni–Sn–P layer, P-rich Ni layer, an amorphous Ni–P deposited layer and Cu pad.

Acknowledgements

This work was supported by grant No. (R01-2000-00227) from the Basic Research of the Korea Science & Engineering Foundation.

REFERENCES

1) R. J. Klein Wassink: *Soldering in Electronics*, 2nd Edn., (Electrochemical Publications Ltd., Scotland, 1989) pp. 1–35.
2) J. R. Oliver, J. Liu and Z. Lai: Proc. International Symposium on Advanced Packaging Materials, (2000) pp. 152–157.
3) I. Shohji, F. Mori and K. F. Kobayashi: Mater. Trans. **42** (2001) 790–793.
4) S.-W. Ricky Lee and J. H. Lau: Soldering and Surface Mount Technol. **10** (1998) 26–31.
5) P. L. Tu, Y. C. Chan, C. W. Tang and J. K. Lai: Proc. of Electronic Components and Technology Conference, (IEEE, 2000) pp. 1369–1375.
6) C. E. Ho, Y. M. Chen and C. R. Kao: J. Electronic Materials **28** (11) (1999) 1231–1237.
7) S.-W. Ricky Lee and J. H. Lau: Circuit World **23** (1996) 16–19.
8) A. Maeda, T. Umemura, Q. Wu, Y. Tomita and T. Abe: Proc. International Symposium on Advanced Packaging Materials, (2000) pp. 135–140.
9) G. Ghosh: Acta Mater. **48** (2000) 3719–3738.
10) C. B. Lee, S. B. Jung, Y. E. Shin and C. C. Shur: Mater. Trans. **42** (2001) 751–755
11) S. C. Hung, P. J. Zheng, S. C. Lee and J. J. Lee: Proc. of the 1999 IEEE/CPMT Int'l Electronic Manufacturing Technology Symposium, (1999) pp. 7–15.
12) R. J. Coyle, A. Holliday, P. Mescher, P. P. Solan, S. A. Gahr, H. A. Cyker, J. K. Dorey and T. I. Ejim: Proc. IEEE/CPMT Int'l Electronics Manufacturing Technology Symposium, (1999) pp. 23–35.
13) F. D. Bruce Houghton: Circuit World **26** (2000) 10–16.
14) Z. Mei, M. Kaufmann, A. Eslambolchi and P. Johnson: Proc. of the 1998 Electronic Components and Technology Conference, (IEEE,1998) pp. 952–961.
15) R. Erich, R. J. Coyle, G. M. Wenger and A. Primavera: Proc. of the 1999 IEEE/CPMT Int'l Electronics Manufacturing Technology Symposium, (1999) pp. 16–22.
16) Z. Mei, P. Callery, D. Fisher, F. Hua and J. Glager: Advances in Electronic Packaging ASME, EEP-vol. 19–2, (1997) pp. 1543–1550.
17) R. J. Coyle and P. P. Solan: Proc. of the 2000 IEEE/CPMT Int'l Electornic Manufacturing Technology Symposium, (2000) pp. 168–177.
18) J. H. Lau: *Ball Grid Array Technology*, (McGraw Hill, Inc., New York, 1995) pp. 400–410.
19) J. W. Jang, P. G. Kim, K. N. Tu, D. R. Frear and P. Thompson: J. Appl. Phys., **85** (1999) 8456–8463.
20) K. N. Tu and K. Zeng: Mater. Sci. Eng. **R34** (2001) 1–58.